Food and Chemical Toxicology 133 (2019) 110749

Contents lists available at ScienceDirect

Food and Chemical Toxicology

journal homepage: www.elsevier.com/locate/foodchemtox

Extraction of phospholipid-rich fractions from egg yolk and development of liposomes entrapping a dietary polyphenol with neuroactive potential

João Bernardo[a], Romeu A. Videira[a], Patrícia Valentão[a], Francisco Veiga[b,c], Paula B. Andrade[a,*]

[a] REQUIMTE/LAQV, Laboratório de Farmacognosia, Departamento de Química, Faculdade de Farmácia, Universidade do Porto, Rua de Jorge Viterbo Ferreira, no. 228, 4050-313, Porto, Portugal

[b] REQUIMTE/LAQV, Group of Pharmaceutical Technology, Faculty of Pharmacy, University of Coimbra, Coimbra, Portugal

[c] Department of Pharmaceutical Technology, Faculty of Pharmacy, University of Coimbra (FFUC), Pólo das Ciências da Saúde, Azinhaga de Santa Comba, 3000-548, Coimbra, Portugal

ARTICLE INFO

Keywords:
Egg yolk
Phospholipids
Liposomes
Flavonoids
Excitotoxicity
Neuroprotection

ABSTRACT

A new protocol to obtain egg yolk phospholipids in ethanol is presented. Rutin-phospholipids nanoliposomes were prepared and characterized. The procedure takes advantage of the different solubility of egg yolk lipids in ethanol and acetone at low temperature, to efficiently obtain a phospholipid-rich fraction of high purity degree. The phospholipid content in the final fraction is 208.65 ± 26.46 μmol/g fresh egg yolk (16%), accounting for ca. 96% of the extract's dry weight. The phospholipid-rich fraction contains cholesterol (0.069–0.082 cholesterol/phospholipid molar ratio), and vestigial amounts of lutein and zeaxanthin (89.24 ± 9.76 and 14.9 ± 2.16 ng/g of fresh egg yolk, respectively). Saturated fatty acids dominate the extracted phospholipids (50% of egg's total yolk phospholipids), the levels of monounsaturated ranging from 20 to 25%, and polyunsaturated up to 35%. Rutin-liposomes, prepared with phospholipid-rich fraction, presented mean diameter < 140 nm, negative surface charge (Zeta potential ~ −13 mV), and entrapment efficiency of rutin up to 87%. In human neuroblastoma cell line SH-SY5Y, rutin-liposomes (lipid 25 μM + rutin 16.7 μM) attenuated glutamate-induced cytotoxicity, in part by reducing the formation of intracellular reactive species, pointing to their potential application as new functional neuroprotective agents.

1. Introduction

Lipids are at the headway of nanotechnology conveyance for nanostructured delivery systems. Noteworthy applications have been accomplished within the fields of cosmetic, pharmaceutical formulations, and novel functional foods (Mishra et al., 2018). In particular, phospholipids (PL) are considered appealing structural platforms for lipid-based nanocarriers of bioactive compounds. Their amphiphilic character and biocompatibility profile, together with their self-organization properties in water systems, allow the production of supramolecular systems with high entrapment efficiency of both lipophilic and hydrophilic compounds. Additionally, these supramolecular systems improve the bioavailability of the encapsulated compounds and can be manipulated to obtain targeted-delivery systems of desired size. Hence, PL offer a plethora of opportunities to support formulations with a large spectrum of applications in food and biomedical fields (Singh et al., 2017). Inherent to their vast field of applications is the demand for safe-approved formulations supported by these building-blocks. Negative outcomes may arise from the lack of standardization and sterility, or even from undesirable trace amounts of extractive organic solvents in the final preparations (Shukla et al., 2017).

Egg yolk is a rather interesting natural source of bioactive compounds, of easy access and at low expenses. In addition, with the recent advances in the areas of animal feeding and nutrition, eggs have a high potential as functional food due to the possibility to produce designer eggs on demand (Surai and Sparks, 2001). However, the partition of lipids from egg yolk, as example the extraction of PL, is significantly hampered by the varied composition of natural supramolecular assemblies of lipids and proteins in this matrix (Anton, 2013). One of the recurrent issue of extracting PL from egg yolk is the traditional utilization of chloroform as solvent (Folch et al., 1957), an organic solvent known by its toxicity at low concentrations (Pimentel et al., 2018). Consequently, its presence in PL extracts, even in residual amounts, hinders their application in conceivable formulations with potential therapeutic and food applications. On the other hand, the extraction protocols themselves are often not adequately versatile, nor viable for

* Corresponding author.
E-mail address: pandrade@ff.up.pt (P.B. Andrade).

https://doi.org/10.1016/j.fct.2019.110749
Received 3 July 2019; Received in revised form 30 July 2019; Accepted 31 July 2019
Available online 01 August 2019
0278-6915/

the scale-up required by industry.

In view of the recent evidence, polyphenols-based therapies at an appropriate stage of neurodegeneration may hold promise to halt neurodegenerative processes and to improve cognitive function, with positive health outcomes (Mendes et al., 2018). Nonetheless, the low brain bioavailability of polyphenols was considered as one of the major pitfalls behind their application, as reported for flavonoids (Andrade et al., 2016). On this basis, the production of liposomes entrapping dietary polyphenols may enhance their bioavailability and reach the cell targets in pharmacological effective concentrations (Vilamarim et al., 2018).

Herein, we propose a new protocol to obtain standardized PL-rich fraction from egg yolk. It takes advantage of ethanol and acetone as solvents, which are compatible with the regulations required for subsequent pharmaceutical and food applications (European Council, 2009), in combination with the temperature effect over the solubility of lipids (Rowe, 1983). This protocol also makes it possible to reuse the ethanol in one step of the procedure, and allows the recovery of other compounds besides PL (i.e., by-products). Additionally, PL-rich fraction is used to produce rutin-liposomes that entrap the flavonoid rutin with high efficiency, and exhibit a relevant ability to protect neuronal cells against the glutamate-induced cytotoxicity *via* oxidative stress.

2. Materials and methods

2.1. Standards and reagents

Ascorbic acid (≥99.0%), butylated hydroxytoluene (BHT), *t*-butyl methyl ether (HPLC grade), cholesterol (≥99.0%), egg lecithin (egg PC; ≥ 99.0%), 2′,7′-dichlorofluorescein diacetate (DCFH-DA), 1,2-dipalmitoyl-*sn*-glycero-3-phosphoethanolamine (DPPE; ≥ 97.0%), L-glutamic acid monosodium salt monohydrate, Hank's balanced salt solution (HBSS), 4-(2-hydroxyethyl)piperazine-1-ethanesulfonic acid sodium salt (HEPES), lutein (≥97.0%), methylthiazolyldiphenyl-tetrazolium bromide (MTT), *n*-hexane, perchloric acid, potassium dihydrogen phosphate, quercetin-3-*O*-rutinoside (rutin) (≥99.0%), sodium chloride, sodium sulphate anhydrous, sulphuric acid, Supelco® 37 component fatty acid methyl esters (FAME) mix (LC08296V), tert-butyl hydroperoxide (tBuOOH) triethylamine, trypsin-EDTA solution (0.05), and zeaxanthin (≥95.0%) were purchased from Sigma-Aldrich (St. Louis, MO, USA). Ammonium molybdate was acquired to May & Baker Ltd. (London, UK). Acetic anhydride and methanol (HPLC grade) were from Merck kGaA (Darmstadt, Germany). Acetic acid, ethanol and methanol (analytical grade) were purchased from Fisher Chemical (Pittsburgh, PA, USA). Acetone was from VWR (Lutterworth, UK). The spectroscopic probe 16-(9-anthroyloxy) palmitic acid (16-AP) was from Molecular Probes, Inc (Plano, Texas). Commercially available eggs (class L) from different batches of the same Portuguese supplier were used. Dulbecco's Modified Eagle Medium:Nutrient Mixture F-12 (DMEM/F12), phosphate balanced salt solution (PBS), heat inactivated foetal bovine serum (FBS), and Pen Strep solution (Penicillin 5000 units/mL; Streptomycin 5000 μg/mL) were obtained from Gibco® (Life Technologies, Invitrogen™; Grand Island, NY, USA). Human neuroblastoma cell line SH-SY5Y (ATCC® CRL-2266™) was from American Type Culture Collection (Manassas, Virginia, USA).

2.2. Extraction and characterization of phospholipid-rich fractions from egg yolk

2.2.1. Extraction procedure

The extraction of PL from egg yolk was performed using ethanol and acetone as extraction solvents, following the flowchart depicted in Fig. 1. Two egg yolks were used in each extraction process, and four independent extractions were performed. This procedure was rationalized considering the distinct solubility exhibited by neutral lipids and ionic PL, at room temperature, in organic solvents with different degrees of polarity, and also taking advantage of the effect caused by the temperature drop to 4 °C on the solubility of lipids, in the above mentioned solvents (Palacios and Wang, 2005; Su et al., 2014). The final fraction, here designated as PL-rich fraction, was stored at −20 °C, as dry extract or as EtOH/MeOH (2:1, *v/v*) solution, and protected from light, until further analysis.

2.2.2. Quantification of phospholipids

The spectrophotometric quantification of PL, in terms of inorganic phosphate, was performed as described elsewhere (Bartlett and Lewis, 1970). Aliquots of each PL-rich fraction were collected and diluted (100 ×) with a solution of EtOH/MeOH (2:1; *v/v*). The diluted samples (25 μL) were dried under nitrogen stream, and then hydrolysed with 0.5 mL of perchloric acid 70%, at 180 °C for 2 h, to release phosphates from PL. Afterwards, 3.3 mL of H_2O, 0.5 mL of ammonium molybdate (0.25 g/10 mL) and 0.5 mL of ascorbic acid (1 g/10 mL) solutions were added to each glass tube, and the mixture was vortexed before incubation at 100 °C, for 10 min, in a water bath.

The absorbance of the resulting phosphomolybdate complexes was determined at 800 nm. The phosphate concentration in each sample was calculated by interpolation of the external standard equation obtained with KH_2PO_4 (0–250 nmol), subjected to the same procedure as the samples (Table 1).

2.2.3. Quantification of cholesterol

The spectrophotometric quantification of cholesterol was achieved by the Liebermann-Burchard procedure (Huang et al., 1961), with minor alterations. Aliquots (25 μL) of the PL-rich fraction in EtOH/MeOH (2:1; *v/v*) were collected to glass tubes, and solvents were evaporated under nitrogen stream. To the dried lipids were added 0.1 mL of acetic acid, and the reaction, at room temperature, was started by the addition of 5 mL of Liebermann-Burchard reagent (120 mL acetic anhydride + 60 mL acetic acid + 20 mL sulphuric acid + 4 g Na_2SO_4). After 30 min, the absorbance of the resulting blue-green complex was determined at 630 nm. The analytical concentrations were calculated by interpolation with external standard equation of cholesterol (0.31–2.50 mg/mL), subjected to the same procedure as the samples (Table 1).

2.2.4. Identification and quantification of carotenoids by HPLC-DAD

Aliquots (250 μL) of PL-rich fraction, in EtOH/MeOH (2:1; *v/v*), were collected and solvents were evaporated under nitrogen stream. Carotenoids were extracted from the dried lipid extracts by adding 10 mL of acetone. The mixture was sonicated, for 15 min, in a water ultrasonic bath (88/320 W, 35 kHz; Bandelin Sonorex Digitec), followed by stirred maceration (45 min, at 600 rpm). The acetone extracts were collected and filtered through nylon membranes (220 nm pore size), and then the solvent was evaporated under reduced pressure. The dried extract was stored at −20 °C until analysis.

To proceed with the identification and quantification of carotenoids, the dried extracts were solubilized in 200 μL of acetone and 20 μL were analysed in a HPLC-DAD system, as detailed elsewhere (Oliveira et al., 2015). Analytical samples were eluted using a C_{30} YMC column (5 μm, 250 × 4.6 mm; YMC, Kyoto, Japan). The mobile phase consisted of methanol (A) and *t*-butyl methyl ether (B), starting with 95% A; the elution followed with a gradient to obtain 70% B at 30 min, finishing with 50% A at 50 min. The flow rate was set at 0.9 mL/min. Chromatograms were recorded at 450 nm and compared with those of the external standards lutein and zeaxanthin. Their content was calculated by interpolation with the respective external standard equation (Table 1).

2.2.5. Separation of phospholipid classes by thin-layer chromatography

PL classes from the PL-rich fractions were separated by thin-layer chromatography (TLC), using silica gel plates (TLC Silicagel 60 F_{254}; Merck KGaA, Germany). Prior to separation, plates were washed with

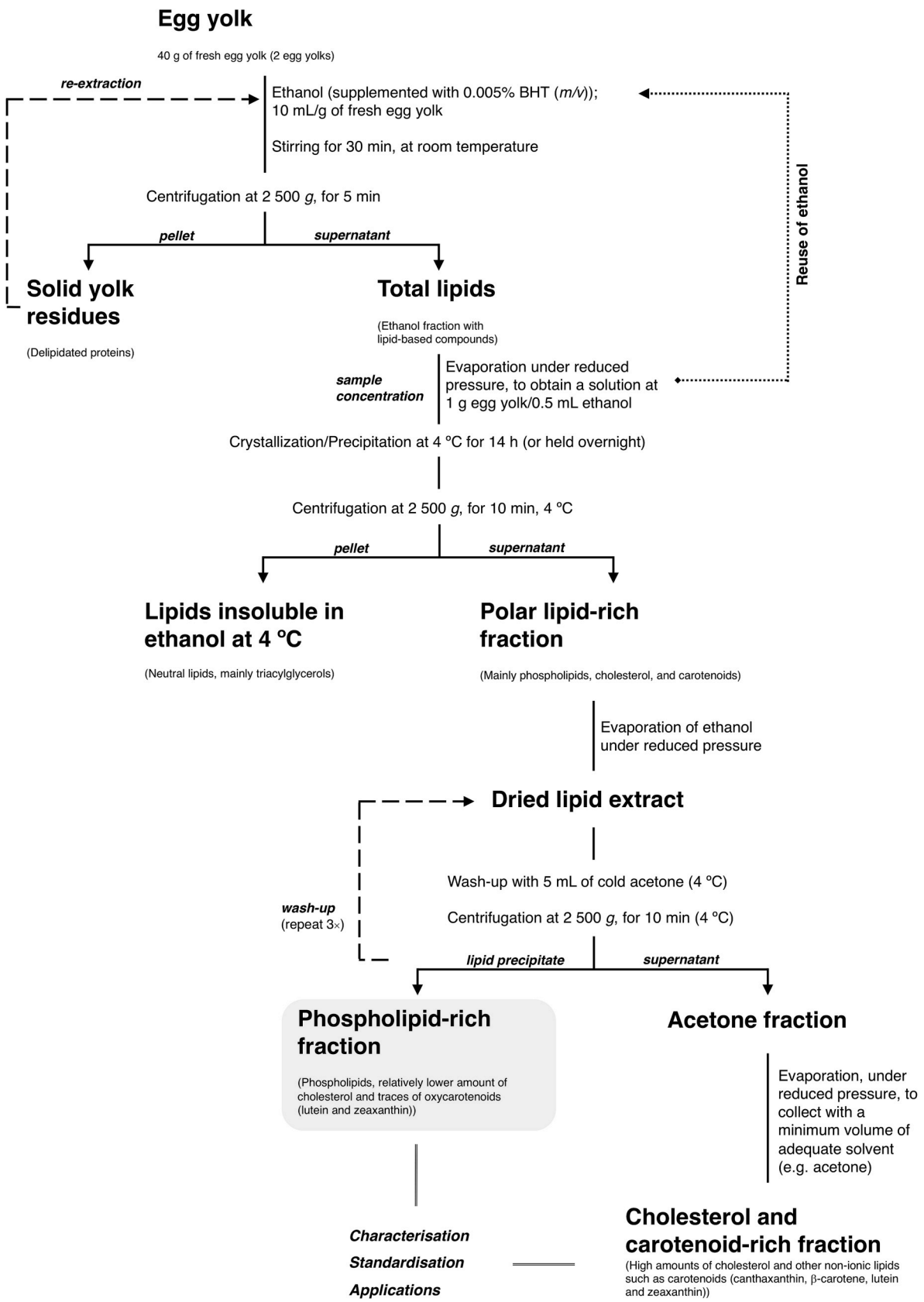

Fig. 1. Flow diagram to obtain a phospholipid-rich fraction from egg yolk, using ethanol and acetone as extractants.

chloroform/methanol (1:1, *v/v*) and treated with boric acid 2.3% in EtOH. The plates with seven independent spots, each one containing 20–30 μg of sample or 5 μg of a standard, were developed in the solvent mixture chloroform:ethanol:water:triethylamine (35:30:7:35, *v/v/v/v*). Lipid spots on TLC were detected at 365 nm, after revelation with primuline (50 μg/100 mL in acetone:water (80:20, *v/v*)). Pure Egg PC and

Table 1
Linear regression equations, limit of detection (LOD) and limit of quantification (LOQ) of the external standards.

	Linear regression	R^2	LOD	LOQ
Phosphates (nmol)	0.0019*x* + 0.0569	0.999	22.579	68.421
Cholesterol (mg/mL)	0.2682*x* + 0.0473	0.999	0.087	0.265
Lutein (mg/mL)	327376*x* + 7.0302	0.999	7.13×10^{-05}	2.16×10^{-04}
Zeaxanthin (mg/mL)	85718*x* + 14.1730	0.999	8.43×10^{-05}	2.55×10^{-04}

DPPE were used as reference standards, since lecithin and phosphatidylethanolamines are the major PL classes in egg yolks.

2.2.6. Preparation of the methyl esters of fatty acyl chains, and profiling by GC-FID

Fatty acid methyl esters (FAME) from the dried lipids extracts were obtained by acid catalysed transmethylation, as previously described (Rosa and Catalá, 1998). Aliquots (900 nmol PL) from each PL-rich fraction were placed in glass tubes, along with 30 μL of the internal standard (IS), fatty acid C_{17} (1 mM, dissolved in chloroform), and dried under a nitric stream. The dried extract was dissolved in 5 mL of freshly prepared HCl/MeOH solution (5%, *v/v*), and incubated in a thermostatic water bath at 70 °C for 2 h. After cooling to room temperature, 5 mL of *n*-hexane were added to each test tube and the mixture was vortexed and centrifuged (3 min, 2000 rpm.). The upper phase, a hexane fraction containing fatty acid methyl esters, was collected and the lower phase was re-extracted with an equal volume of *n*-hexane. The combined fractions were mixed with 6 mL of H_2O and subjected to a new centrifugation step (3 min, 2000 rpm). Next, the aqueous phase was discharged and the water remaining in the hexane phase was removed by the addition of sodium sulphate anhydrous (c.a. 1 g). Finally, the solution was filtered, and the solvent evaporated to dryness under reduced pressure. The extracted methyl esters were solubilized with 200 μL of *n*-hexane and stored at −20 °C, until analysis.

The fatty acid profiling by GC-FID was carried out in a Finnigan Focus GC apparatus (Thermo Fisher Scientific, Waltham, MA, USA) equipped with a flame ionization detector and a VF-5 ms column (30 m × 0.25 mm × 0.25 μm) (Varian BV, Middelburg, The Netherlands), and the injection volume was of 1 μL (derivatized lipid extracts containing the IS, and FAME mixture). The carrier was high purity helium C-60 (Gasin, Portugal) at constant 1 mL/min flow rate. Temperatures of the injector and detector were maintained at 250 °C. The oven temperature was set at 40 °C for 1 min, then increased 5 °C/min to 250 °C, 3 °C/min to reach 300 °C and held for 15 min. The compounds were identified by comparing their retention times with the FAME mixture, and their contents calculated as relative % of the internal standard $C_{17:0}$.

2.3. Production and characterization of nanoformulations

All nanoformulations were prepared by thin film hydration method. Aliquots of the PL-rich fractions (PL 2.5 mM) were collected and dissolved in 5 mL of EtOH/MeOH (2:1, *v/v*) in round-bottom flasks. To prepare liposomes, solvents were evaporated to dryness and the resulting dry thin lipid film was hydrated with 10 mL of HEPES solution (NaCl 50 mM + HEPES 10 mM; pH 7.0). Then, the mixture was subjected to sonication cycles (2 min) alternate with hand shaking (2 min), in a total of 20 min, at controlled temperature (37 °C). The suspensions of small unilamellar vesicles were manually extruded through polycarbonate membranes (200 nm pore size).

Liposomes entrapping rutin were prepared by supplementing HEPES solution with this flavonoid to obtain final formulations of 250 μM, 125 μM, 63 μM and 31 μM. Non-encapsulated rutin was removed by dialysis, for 18 h, through a cellulose membrane (cut-off 14 kDa; Sigma-Aldrich). The formulations were collected in sterilized vials and stored (4 °C) until further analysis.

2.3.1. Entrapment efficiency

The entrapment efficiency (EF), here representing the amount of rutin incorporated into liposomes, was determined at the absorption maxima of 350 nm in a Unicam Helios Alpha UV–Visible spectrophotometer (Thermo Spectronic, Cambridge, UK), and according with the equation: $EF\ (\%) = \frac{Abs\ liposomes\ post - dialysis}{Abs\ liposomes} \times 100$.

2.3.2. Particle size and zeta potential

All samples were diluted in HEPES buffer (1:4) to yield a suitable scattering intensity (count rate between 300 and 500 kcps). Particle size, size distribution and polydispersity index (PDI) were obtained by dynamic light scattering in a particle size analyser (Brookhaven Instruments, Holtsville, NY, USA). Individual running time was of 120 s, and 6 runs *per* each measurement were performed.

Zeta potential was determined by electrophoretic light scattering (ELS), using a ZetaPALS instrument (Brookhaven Instruments, Holtsville, NY, USA). Data recorded from six runs (10 cycles *per* run) with a relative residual value (measure of data fit quality) of 0.03.

2.3.3. Incorporation of 16-AP probe in liposomes, and determination of the partition coefficient of rutin

The 16-AP probe (final concentration of 0.65 μM) was added to previously prepared liposome suspensions of 100, 300, 400 and 600 μM lipid. To promote the incorporation of 16-AP into the lipid bilayers, the mixtures were placed under magnetic stirring for 4 h at 37 °C, protected from light exposure. Then, aliquots of each liposome suspension were collected and added with rutin, prepared in HEPPES buffer, to obtain the final molarities of 0, 1, 3, 8, 21, 35 and 50 μM, while keeping the lipid molarity constant. The mixtures were again subjected to magnetic stirring for 4 h at 37 °C.

The location of rutin within the liposome lipid bilayer and its lipid-water partition were determined by its quenching effect on the fluorescence of 16-AP. The fluorescence emission spectra of 16-AP (λ_{exc} = 360 nm), in the absence and presence of rutin, was acquired between 390 and 650 nm. The lipid-water partition coefficient was determined from the Stern-Volmer modified equation, as before (Fato et al., 1986), following the equation: $\frac{1}{Kapp} = \left(\frac{1}{Kq} - \frac{1}{KqKp}\right)\alpha m + \frac{1}{KqKp}$, where K_{app} is the apparent quenching constant determined experimentally by Stern-Volmer plots, K_q is the biomolecular quenching constant for rutin in the membrane, K*p* is the partition coefficient, and α_m is the volume fraction of the membrane phase assuming a lipid-specific volume of 0.984 μL/mg of lipid (White et al., 1987).

2.4. Cell culture and assays

SH-SY5Y cells were cultured in DMEM/F12 supplemented with FBS (10%) and Pen-Strep (1%), at 37 °C, with 5% CO_2 humidified atmosphere (Toreuse model 2428; Saint Louis, Missouri, USA).

2.4.1. SH-SY5Y cytotoxicity induced by glutamate

SH-SY5Y cells were seeded at 40 000 cells/well in 96-wells plates. The rutin-liposome formulations were diluted with culture medium (10 ×) and then sterilized through 0.22 μm pore filters. The effect of rutin-liposomes (lipid 25 μM + rutin 16.7 μM; concentration of rutin predicted by the entrapment efficiency) and glutamate on the viability of SH-SY5Y cells was evaluated after 24 h of incubation. The protective effect of rutin-liposomes against glutamate-induced cytotoxicity was evaluated by pre-incubating the cells with the formulation alone for 2 h, followed by a period of 22 h of co-exposition to glutamate (50 mM).

2.4.2. MTT viability assay

After the incubation periods, the growth medium was removed and replaced by MTT solution (0.5 mg/mL, 2 h), and then the absorbance was determined at 510 nm in a microplate reader (Thermo Spectronic, Cambridge, UK). The results were compared with the respective controls.

2.4.3. Determination of intracellular reactive species

The determination of intracellular reactive species was carried out as before (Bernardo et al., 2017), with minor modifications. Briefly, SH-SY5Y cells were seeded at 40 000 cells/well in 96-wells dark plates, and after 24 h they were incubated with DCFH-DA (25 mM, 1 h). The over plus of fluorescent probe was washed out with HBSS, and then cells were pre-incubated for 2 h with rutin-liposomes (lipid 25 μM + rutin 16.7 μM). The toxic stimulus was induced by glutamate (50 mM) over 1 h, with and without previous exposition to rutin-liposomes. The fluorescence (λ_{exc} = 485 nm; λ_{emi} = 535 nm) was recorded in a microplate fluorimeter (SynergyTM H1, Biotek Instruments Winooski, USA). The results were compared with the respective controls.

2.5. Data and statistical analysis

The PL-rich fractions were obtained from four independent extractions, each one starting from two egg yolks of different egg batches. Three aliquots of every PL-rich fraction were collected and characterized, and results expressed as mean ± standard deviation (SD) of three independent determinations. TLC plates were developed with aliquots of each PL-rich fraction. Entrapment efficiency, Zeta potential and particle size were determined for three independent formulations. At least three experiments, each performed in triplicate, were conducted for cellular assays and results were expressed as mean ± SD. A one-way ANOVA followed by Tukey's *post hoc* was applied (level of statistical significance $p < 0.05$).

3. Results and discussion

3.1. An improved procedure to obtain egg yolk phospholipids for food and pharmaceutical applications

The partition of egg yolk bioactive compounds in any solvent system is significantly hampered by the organization of supramolecular assemblies of lipids and proteins within the yolk. When a PL-directed extraction is intended, it becomes necessary, right at the outset, to separate lipids from yolk proteins, including from those with high-affinity for lipids (i.e., disassembling the lipoproteins) (Gładkowski et al., 2012), and then separate PL from the other lipids.

To overcome this issue, it was outlined a multi-step procedure to obtain egg yolk PL in a PL-rich fraction, using two solvents approved for food applications, namely ethanol and acetone, as depicted in Fig. 1. Ethanol is used uppermost to disassemble lipoproteins and to promote protein delipidation and precipitation, thus allowing efficient extractions with high yields (Su et al., 2014). With this first step, the total lipids are collected in the ethanol fraction. At the same time, the solid yolk residue, dominated by aggregates of denaturised proteins, can be collected by centrifugation (2500 *g*, 5 min) and be used for re-extraction, or simply discarded. The ethanol fraction is then concentrated by evaporation under reduced pressure, in order to obtain a solution of extractable lipids at 1 g egg yolk/0.5 mL ethanol.

This concentrated complex mixture of egg yolk lipid-base compounds, containing 240 ± 10.50 μmol of PL/g fresh egg yolk, is further submitted to crystallization/precipitation for 14 h, at 4 °C. The temperature drop triggers the crystallization and/or precipitation of the lipids with lower solubility in cold ethanol (e.g., neutral lipids), such as triacylglycerols (Nielsen and Shukla, 2004), which can be collected by centrifugation. On the other hand, polar lipids, including PL, cholesterol and carotenoids, remain soluble in the supernatant (ethanol), here designated as polar lipid-rich fraction (Fig. 1). In this step, it was taken advantage from the distinct solubility of different groups of lipids in cold ethanol to discard the neutral ones. Notably, in the next step, it is the distinct solubility of polar non-ionic lipids and ionic lipids in cold acetone that enables to obtain PL (ionic lipids) in a spared fraction (Gładkowski et al., 2012).

With the evaporation of ethanol followed by wash-up cycles with cold acetone (4 °C) is obtained a lipid precipitate, collected by centrifugation, which is mainly constituted by PL and herein designated as PL-rich fraction (Fig. 1). The cold acetone solubilizes the triacylglycerol surplus, high amounts of cholesterol and other non-ionic lipids, such as carotenoids (canthaxanthin, β-carotene, lutein and zeaxanthin). By these means, it is obtained a cholesterol and carotenoid-rich fraction after acetone evaporation (Fig. 1). In contrast, the resulting PL-rich fraction has a significantly lower amount of cholesterol, and traceable lutein and zeaxanthin, more polar oxycarotenoids, as revealed by the chemical characterization described below.

3.2. Chemical characterization of the phospholipid-rich fraction

Four PL-rich fractions, obtained from independent egg yolks, were characterized considering their PL profile (total content and fatty acid composition), cholesterol content and carotenoid profile (identification and quantification of molecular species), in order to evaluate the efficiency of the process and the degree of purity of the final extract.

3.2.1. Phospholipids and fatty acids

Data in Table 2 indicate that the extraction procedure is efficient, translated into high yields along with a high degree of reproducibility, as demonstrated by the narrow variation of the PL content of the four independent samples analysed (208.65 ± 26.46 μmol/g fresh egg yolk).

Additionally, PL account for approximately 96% of the PL-rich fraction dry weight; when expressed as percentage of fresh egg yolk weight, the mean of extraction yield was around 16%. These findings fit our goals, since similar results were reported when applying a multi-step protocol for an exhaustive large-scale extraction of PL from egg yolk using ethanol and hexane (Palacios and Wang, 2005). However, the utilization of hexane as extractant is a disadvantage, since putative residual amounts of this solvent confer toxic risk to the final products (European Council, 2009). A more efficient egg yolk PL extraction yield (~30%) was reported by using a protocol with ethanol to extract total lipids, a precipitation step at low temperatures to discard neutral lipids, and β-cyclodextrin to remove cholesterol (Su et al., 2014). Nonetheless, the success of this methodology is dependent of a step that requires temperatures close to 50 °C and the use of β-cyclodextrin. Therefore, this step entails higher expenses than our proposed procedure; likewise, it significantly increases the risk of the polyunsaturated fatty acids present in egg yolk PL to undergo oxidation, which has a negative impact in food and pharmacological applications.

Apart from validating the efficiency of the process, it is also important to characterize the PL profile of the final fraction. Egg yolk PL have been extensively explored, being mainly constituted by phosphatidylcholine (PC) and phosphatidylethanolamine (PE), accounting up to 76 and 22% of total PL, respectively (Anton, 2013). Trace amounts of

Table 2
Characterization of the four-individual phospholipid-rich fractions (normalized to fresh egg yolk weight), each obtained through independent extractions.

	Extraction number				
	1	2	3	4	Mean ± SD[c]
Fresh egg yolk weight (g)	37.566	38.710	36.388	39.596	38.065 ± 1.393
Phospholipids (μmol/g fresh egg yolk)[a]	222.80 ± 6.21 (18%)[b]	184.33 ± 10.04 (15%)[b]	188.67 ± 3.06 (15%)[b]	238.81 ± 8.11 (17%)[b]	208.65 ± 24.74 (16%)
Cholesterol (μmol/g fresh egg yolk)[a]	16.95 ± 3.71	13.38 ± 0.55	13.08 ± 0.55	19.57 ± 1.12	15.75 ± 3.27
Lutein (ng/g fresh egg yolk)[a]	15.52 ± 1.29	16.34 ± 4.31	16.14 ± 0.38	11.73 ± 4.34	13.81 ± 2.48
Zeaxanthin (ng/g fresh egg yolk)[a]	91.07 ± 9.40	98.46 ± 1.67	91.98 ± 6.33	75.46 ± 5.13	88.33 ± 11.75
Cholesterol/phospholipid molar *ratio*	0.076	0.073	0.069	0.082	0.075 ± 0.005
Molar fraction of cholesterol (%)	7.07	6.77	6.48	7.57	6.97 ± 0.47

[a] Expressed as mean ± SD, calculated from determinations of three aliquots of each independent extraction.
[b] % of extraction = (phospholipid (g)/fresh egg yolk (g) × 100).
[c] Calculated considering all the single determinations.

lysoPC and lysoPE, phosphatidylinositol, phosphatidylserine, sphingomyelin, or cardiolipins can also be found in egg yolk lipid extracts.

In this work, the qualitative analysis of each final PL-rich fraction was performed by TLC (data not shown). In the thin-layer separation were clearly visible two major spots with retardation factors similar to those of EggPC and DPPE. As expected, this suggests that PC and PE are also the main PL classes in the PL-rich fraction. In addition, spots with minor intensity were also detectable, which may correspond to the traceable PL classes present in egg yolk.

The fatty acid composition of the extracted PL was also evaluated, since it has biological relevance for further uses of these PL-rich fractions in food and pharmaceutical industries. It is well-documented that the fatty acid composition of the egg yolk PL can be modulated by the diet given to the hens, which has particular impact on the relative abundance of polyunsaturated fatty acids (PUFA) and monounsaturated fatty acids (MUFA), as well as in the *n*-6/*n*-3 PUFA molar *ratio* (Du et al., 1999). In general, saturated fatty acids (SFA) account for 45–50% of egg yolk PL, while the MUFA levels range between 20 and 25%, and PUFA can reach up to 35% (Anton, 2013).

Fig. 2 and Table 3 show the fatty acid profile of the PL found in the final fractions obtained by the proposed procedure. Thirteen fatty acids were identified and quantified, comprising four SFA, two MUFA and seven PUFA.

Despite the wide diversity of PUFA molecular species, SFA palmitic

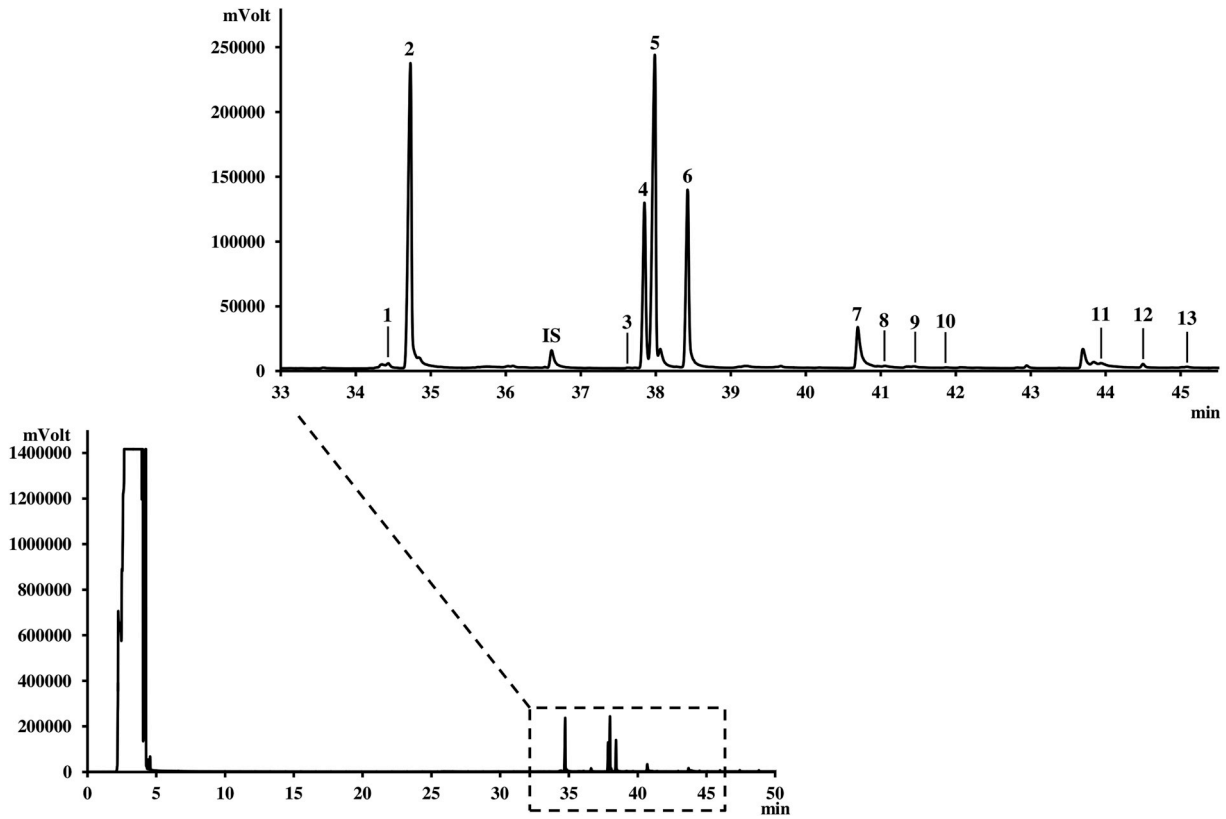

Fig. 2. Representative GC-FID chromatogram of the fatty acid composition of phospholipids extracted from egg yolk, after acid hydrolysis. **(1)** $C_{16:1}$; **(2)** $C_{16:0}$; **(3)** $C_{18:3\ n\text{-}3}$; **(4)** $C_{18:2\ n\text{-}6}$; **(5)** $C_{18:1}$; **(6)** $C_{18:0}$; **(7)** $C_{20:5\ n\text{-}3}$; **(8)** $C_{20:3\ n\text{-}3}$; **(9)** $C_{20:2\ n\text{-}6}$; **(10)** $C_{20:0}$; **(11)** $C_{22:6\ n\text{-}3}$; **(12)** $C_{22:2}$; **(13)** $C_{22:0}$; **(IS)** Internal standard $C_{17:0}$.

Table 3
Fatty acid composition of the four phospholipid-rich fractions.

Fatty acid[a]	Extraction number				
	1	2	3	4	Mean ± SD[b]
$C_{16:1}$	1.04	0.69	0.84	0.94	0.88 ± 0.15
$C_{16:0}$	31.70	31.04	32.94	31.94	31.91 ± 0.79
$C_{18:3\ n\text{-}3}$	0.10	0.06	0.10	0.05	0.08 ± 0.03
$C_{18:2\ n\text{-}6}$	12.90	12.83	11.84	12.59	12.54 ± 0.49
$C_{18:1}$	25.32	30.99	25.86	29.60	27.94 ± 2.78
$C_{18:0}$	21.39	16.77	18.26	16.58	18.25 ± 2.22
$C_{20:5\ n\text{-}3}$	5.68	5.45	5.60	5.15	5.47 ± 0.23
$C_{20:3\ n\text{-}3}$	0.26	0.53	0.59	0.78	0.54 ± 0.21
$C_{20:2\ n\text{-}6}$	0.01	0.13	0.17	0.19	0.13 ± 0.08
$C_{20:0}$	0.18	0.11	0.31	0.14	0.19 ± 0.09
$C_{22:6\ n\text{-}3}$	0.91	0.83	0.87	0.99	0.90 ± 0.07
$C_{22:2}$	0.09	0.37	1.55	1.37	0.85 ± 0.72
$C_{22:0}$	0.43	0.19	0.98	0.53	0.53 ± 0.33
Σ SFA (%)	~54	~48	~52	~48	51 ± 3
Σ MUFA (%)	~26	~32	~27	~31	29 ± 3
Σ PUFA (%)	~20	~20	~21	~21	20 ± 1
n-6/*n*-3 PUFA *ratio*	1.9	1.9	1.7	1.8	1.8 ± 0.1

[a] Mean of determinations of three independent derivatizations obtained from each phospholipid-rich fraction, expressed as relative % of the internal standard $C_{17:0}$.
[b] Calculated considering all single determinations.

acid ($C_{16:0}$) was always the one with the highest relative abundance (31.91 ± 0.79%), followed by stearic acid ($C_{18:0}$; relative abundance of 18.25 ± 2.22%). Consequently, the fatty acid profile of the extracted egg yolk PL is dominated by saturated fatty acids representing ~51% of the total content. As for the other fatty acid classes, total MUFA represent around 29% of the fatty acid content of the extracted PL, oleic acid ($C_{18:1}$) being much more abundant than palmitoleic acid ($C_{16:1}$) (Table 3). On the other hand, PUFA represent 21% of the PL fatty acid content; among those, linoleic acid ($C_{18:2\ n\text{-}6}$) is the more representative of $_{n\text{-}6}$ PUFA series, and eicosapentaenoic acid ($C_{20:5\ n\text{-}3}$) dominates within the $_{n\text{-}3}$ PUFA. The *n*-6/*n*-3 PUFA *ratio* calculated for the PL-rich fraction is 1.8 ± 0.1 (Table 3).

This fatty acid profile complies with previously reported data (Du et al., 1999), suggesting that the PL-rich fraction is dominated by membrane PL. In general, the PL of PC and PE classes exhibit a saturated fatty acid in *sn*-1 position and a monounsaturated or a polyunsaturated fatty acid in the *sn*-2 position of the glycerol, promoting profiles with 50% of saturated fatty acids. It was already reported that in the fatty acid profile of egg yolk PC, approximately 33% are C_{16}, 14–20% are saturated C_{18}, and around 40% are unsaturated C_{18} (mainly oleic acid) (Hawke, 1959). These results also sustain that triglycerides were removed during the extraction procedure (Fig. 1), since their fatty acid distribution contents is of approximately 60% of oleic ($C_{18:1}$) and linoleic ($C_{18:2}$) acids (Parkinson, 1966).

3.2.2. Cholesterol content of the phospholipid-rich fraction – the major contaminant

In general, protocols implementing the sequential partition of egg yolk lipids are delineated to obtain PL extracts of maximum purity by discarding the unwanted by-products, such as cholesterol. Nonetheless, cholesterol itself plays a strategic role in the functional organization of biological membranes and also in the PL-based formulations. In fact, the lateral organization of PL (e.g. membranes rafts dynamics), fatty acyl chain fluidity, membrane permeability and the partition of lipophilic drugs are dependent upon the relative levels of cholesterol (Videira et al., 1999). Thus, cholesterol levels higher than 10% are commonly used in lipid-based formulations to increase the drug encapsulation efficiency, to improve the stability of the vesicles, or even to obtain a most favourable drug release pattern within the biological systems (Briuglia et al., 2015).

The total cholesterol content in the PL-rich fraction is displayed in Table 2. The relative abundance of cholesterol, expressed as molar percentage, ranged between 6.48 and 7.57%; the cholesterol/PL molar *ratio* varied between 0.069 and 0.082. Thus, the extraction protocol exhibits good reproducibility and the levels of cholesterol are relatively low, suggesting that the PL-rich fraction can be used, without further purification steps, to prepare lipid-based formulations for food and pharmacological applications. However, it is also important to stress that the cholesterol content in the PL-rich fraction can be adjusted, if and when necessary, by increasing or reducing the number of precipitation/wash-up steps with cold acetone (Fig. 1), representing an additional advantage of the proposed methodology.

3.2.3. Lutein and zeaxanthin content – minor contaminants

The chemical characterization of the PL-rich fractions, obtained from egg yolks by the proposed protocol (Fig. 1), would not be complete without considering its content of carotenoids. In fact, egg yolk carotenoids, likewise cholesterol, are considered by-products and undesirable impurities of the PL-pure extracts; notwithstanding, their presence in lipid nanostructures may constitute a valuable asset.

The HPLC-DAD analysis of the PL-rich fraction revealed trace amounts of two oxycarotenoids, lutein and zeaxanthin (Fig. 3A).

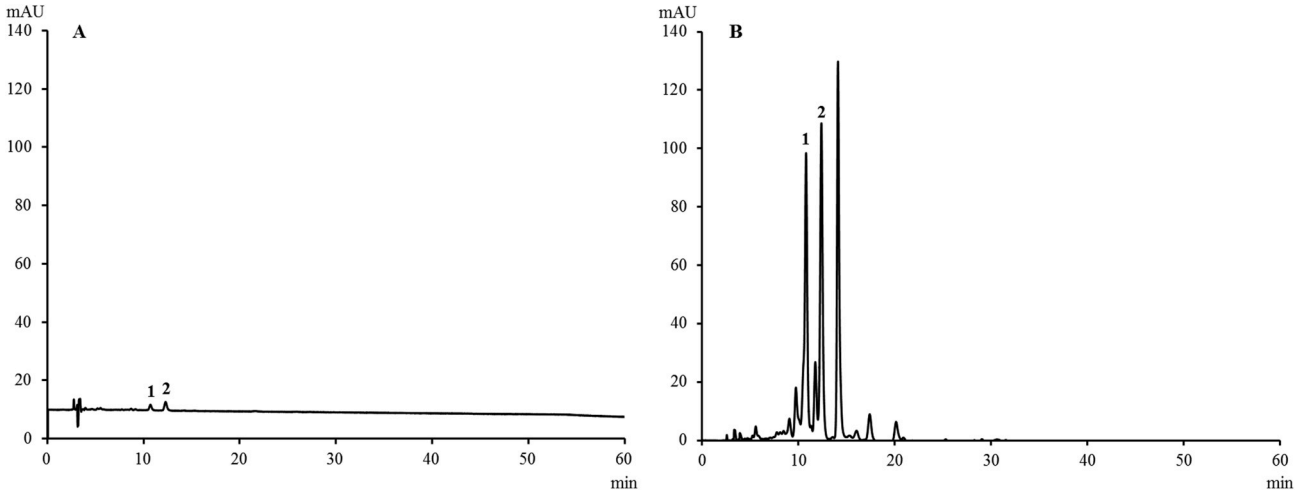

Fig. 3. Representative HPLC-DAD chromatograms (at 450 nm) of the carotenoids in the phospholipid-rich fractions (**A**), and in the collected acetone fractions (**B**). **(1)** Lutein; **(2)** Zeaxanthin.

Similar levels of these two xanthophylls were found in the final fraction, obtained from four independent egg yolk samples, supporting again the reproducibility of this extraction protocol. Zeaxanthin was the one present at higher concentration, followed by lutein, with respective mean ± SD values of 89.24 ± 9.76 and 14.93 ± 2.16 ng/g of fresh egg yolk (Table 2). Systematically, lutein is described as dominant carotenoid in egg yolk in a 2:1 *ratio* relative to zeaxanthin (Schlatterer and Breithaupt, 2006); the same *ratio* was found in the final lipid extracts when the egg yolk was fractionated with ethanol and hexane, but the ethanolic extraction of zeaxanthin was demonstrated to be more efficient than the one of lutein (Kovalcuks and Duma, 2016). Therefore, we assume that our results can be explained, at the same time, by the low temperature effect and the distinct solubility of xanthophylls in ethanol/acetone.

Carotenoids, and their enzymatic cleavage products, are associated with diverse biological processes with a positive impact to human health, and are widely implemented in industry as food ingredients, additives or supplements (Rodriguez-Concepcion et al., 2018). Their broad versatility also verses their application in nanotechnology, either by encapsulation in liposomes to enhance their biological activities (Tan et al., 2014), or by the impact of the carotenoid–lipid interactions on the dynamics of the lipid bilayers (Popova and Andreeva, 2013). As extensively reviewed, polar carotenoids, such as lutein and zeaxanthin, are proved modifiers of the structural and dynamic properties of PL membranes, which ultimately will decrease the quality of liposome products, by spanning lipid bilayers with their polar groups anchored in opposite zones of the membrane; they favour the stiffness of the fluid phase of the PL membranes due to the van der Waals interactions with the acyl chains of lipids; they limit oxygen penetration and act as antioxidants, hence preventing chemical degradation reactions by the hydrolysis of the ester bonds linking the fatty acids to the glycerol backbone and the peroxidation of unsaturated acyl chains (Gruszecki and Strzałka, 2005).

As for the other characteristic carotenoids of egg yolk, such as canthaxanthin, β-carotene, capsanthin, β-cryptoxanthin, among others (Schlatterer and Breithaupt, 2006), they were not identified in these PL-rich fractions (Fig. 3A). For the majority of carotenoids, non-ionic lipids, it is expected a more efficient qualitative and quantitative extraction with a relatively less polar solvent (acetone), rather than with a polar one (ethanol). In fact, this is confirmed by the HPLC-DAD analysis of the acetone fractions, which revealed the presence of numerous peaks corresponding to carotenoids, lutein and zeaxanthin being found among them (Fig. 3B). Apart from the main goal, and since acetone fractions can be collected and preserved, these by-products can be latter separated and redirected towards multiple applications.

3.3. Application of phospholipid-rich fractions as building-block material for rutin-liposomes

The standardized egg yolk PL-rich fraction can be used as main ingredient in several types of commercial lipid-based products, including in the smart nano-systems used to deliver pharmacological drugs and nutraceuticals. Acting as nootropic formulations, they are intended to entrap bioactive compounds, such as flavonoids, and deliver them to the CNS in biological effective concentrations to modulate neurological processes. In this work, rutin was selected as model-compound to be entrapped in liposomes, once it is widely found in the diet (Gullón et al., 2017) and exhibits a bioactivity with potential to promote positive impacts on degenerative brain diseases (Enogieru et al., 2018).

3.3.1. Entrapment efficiency (EE), size distribution and zeta potential

The EE was assessed as function of the variation of rutin loading concentration (32, 63, 125 and 250 μM), setting the PL molarity constant (2.5 mM). The absorbance of formulations was recorded before and after dialysis at 350 nm, which corresponds to the wavelength of maximum absorbance of rutin. In these experimental conditions, the amount of rutin entrapped in liposomes increases linearly with increasing bulk flavonoid concentration in the buffer solution used to prepare the liposomes (Table 4). However, the EE decreases with increasing PL:rutin molar *ratios*, reaching its maximum (87.0 ± 0.9%) at 80:1 M *ratio* (lowest *ratio* tested). In fact, data of EE (Table 4) suggest that the encapsulation of rutin in liposomal formulations follows a saturation curve, as reported for other flavonoids (Huang et al., 2017).

Besides the EE, the mean particle size and zeta potential of the nanoformulations are also affected by the amount of rutin intercalated within the lipid membranes. The control liposomes present a mean particle size of 101.0 ± 8.2 nm, while liposomes entrapping rutin, at all loading concentrations, display higher values (Table 4). This phenomenon was observed for other liposomes loaded with flavonoids, in particular for the parent aglycone quercetin (Huang et al., 2017). In terms of zeta potential, as the rutin entrapped concentration increases, the surface charge is progressively more negative (Table 4). Since strong electronegative values are normally predictive of stable nanoformulations (Müller et al., 2001), these results indicate that the entrapment of rutin improves the physical stability of liposomes.

3.3.2. Interaction of rutin with liposome membranes

The characterization of rutin-lipid membrane interactions is an essential issue to understand how different parameters, including size, formulation stability and surface charge, modulate its biological activity. Thus, partition coefficient of rutin between water and lipid membranes, as well as their preferential localization across the bilayer thickness, were investigated by fluorescence quenching methods, using the 16-AP membrane probe. In liposomes, the 16-AP molecule has a preferential vertical orientation, and its anthroyloxy moiety is located deeply in the hydrocarbon region of the phospholipid bilayer (Handa et al., 1987). Therefore, if a molecule directly changes the fluorescence characteristics of this environment-sensitive fluorophore (i.e. maximum wavelength, fluorescence intensity or lifetime), then it penetrates the phospholipid bilayer, thus being located close to the hydrophobic core.

In Fig. 4 is demonstrated that the fluorescence intensity of 16-AP decreases with increasing concentrations of rutin up to 50 μM, suggesting that the flavonoid is deeply incorporated in the lipid bilayer. Thus, rutin interacts with phospholipid hydrophobic chains, despite its 3-*O*-rutinose polar substitution. Moreover, the fluorescence quenching data can be described by Stern-Volmer equation, and the reciprocal of the apparent Stern-Volmer constant ($1/K_{app}$) increases linearly with the increasing volume of lipid membranes (from 100 to 600 μM in phospholipid), allowing the determination of the partition coefficients (K_p) for rutin (table insert in Fig. 4). The highest K_p value obtained for rutin ($K_p = 1230 \pm 187$) indicates that the flavonoid is preferentially accumulated into the hydrophobic core of the lipid membrane. Therefore, it is able to promote changes in the lipid packing order and membrane fluidity with positive impact on the stability of liposomes and surface charge, as previously suggested for other flavonoids (Arora et al., 2000).

Taking this data in consideration, we may assume that the liposomes produced with the egg yolk PL-rich fraction are a valuable platform to entrap other polyphenols, besides rutin, or even phenolic-rich extracts obtained from medicinal species.

3.3.3. Rutin-liposomes attenuate SH-SY5Y excitotoxicity induced by glutamate long exposure

In Human brain, glutamate is the major excitatory neurotransmitter, and the exacerbation of its stimuli triggers a phenomenon described as excitotoxicity, which is associated with a wide range of acute and chronic neurodegenerative disorders (Cassano et al., 2016). For this reason, any strategies to reduce the glutamate toxicity or to modulate the mitochondrial related damage may be of great value.

In this work, the extent of glutamate-induced toxicity in the SH-SY5Y neuronal model was evaluated by MTT reduction assay, which

Table 4
Entrapment efficiency (EE), mean particle size, polydispersity index (PDI), and zeta potential of liposome formulations.

	EE (%)[a]	Mean particle size (nm)[a]	PDI[a]	Zeta potential (mV)[a]
Liposomes		101.0 ± 8.2	0.259 ± 0.080	−5.72 ± 0.70
Liposomes + Rutin 250 μM	66.8 ± 2.0 (167 μM)[b]	138.2 ± 30.4	0.286 ± 0.006	−13.19 ± 2.45
Liposomes + Rutin 125 μM	68.6 ± 2.1 (86 μM)[b]	133.2 ± 12.1	0.305 ± 0.007	−12.98 ± 2.65
Liposomes + Rutin 63 μM	80.0 ± 1.4 (50 μM)[b]	138.0 ± 12.6	0.293 ± 0.007	−11.39 ± 2.93
Liposomes + Rutin 32 μM	87.0 ± 0.9 (28 μM)[b]	128.3 ± 10.0	0.290 ± 0.005	−10.09 ± 2.83

[a] Results represent the mean ± SD from three independent formulations.
[b] Final concentration of rutin entrapped in liposomes as predicted by the EE.

reflects mitochondrial activity. Our results demonstrate that rutin-liposomes do not alter the cell viability after a 24 h incubation period (Fig. 5A).

As for glutamate (50 mM), as expected, it was responsible for lowering cell viability to approximately 60% of the controls ($p < 0.01$), after a 22 h incubation period. However, under the same conditions, when the cells were pre-incubated for 2 h with the rutin-liposomes (lipid 25 μM + rutin 16.7 μM) and then co-exposed to glutamate for 22 h, the final toxic effect of glutamate was significantly reduced ($p < 0.01$) (Fig. 5A). This suggest that rutin-liposomes attenuate the glutamate-induced excitotoxicity, here translated into a less extended cell death.

Glutamate excitotoxicity, the loss of mitochondrial performance and increased oxidative stress are some of the interconnected key-elements in neurodegenerative processes (Atlante et al., 2001). For this reason, the effect of rutin-liposomes over the formation of intracellular reactive species was also explored. When cells are exposed to glutamate (50 mM, 1 h) it triggers an increase of ~43% of intracellular reactive species (Fig. 5B). However, this effect is less pronounced when the cells are pre-incubated for 2 h with rutin-liposomes (lipid 25 μM + rutin 16.7 μM), as observed by the reduction to ~ 18% of the produced reactive species (Fig. 5B). In fact, rutin-liposomes alone tend to counteract the basal

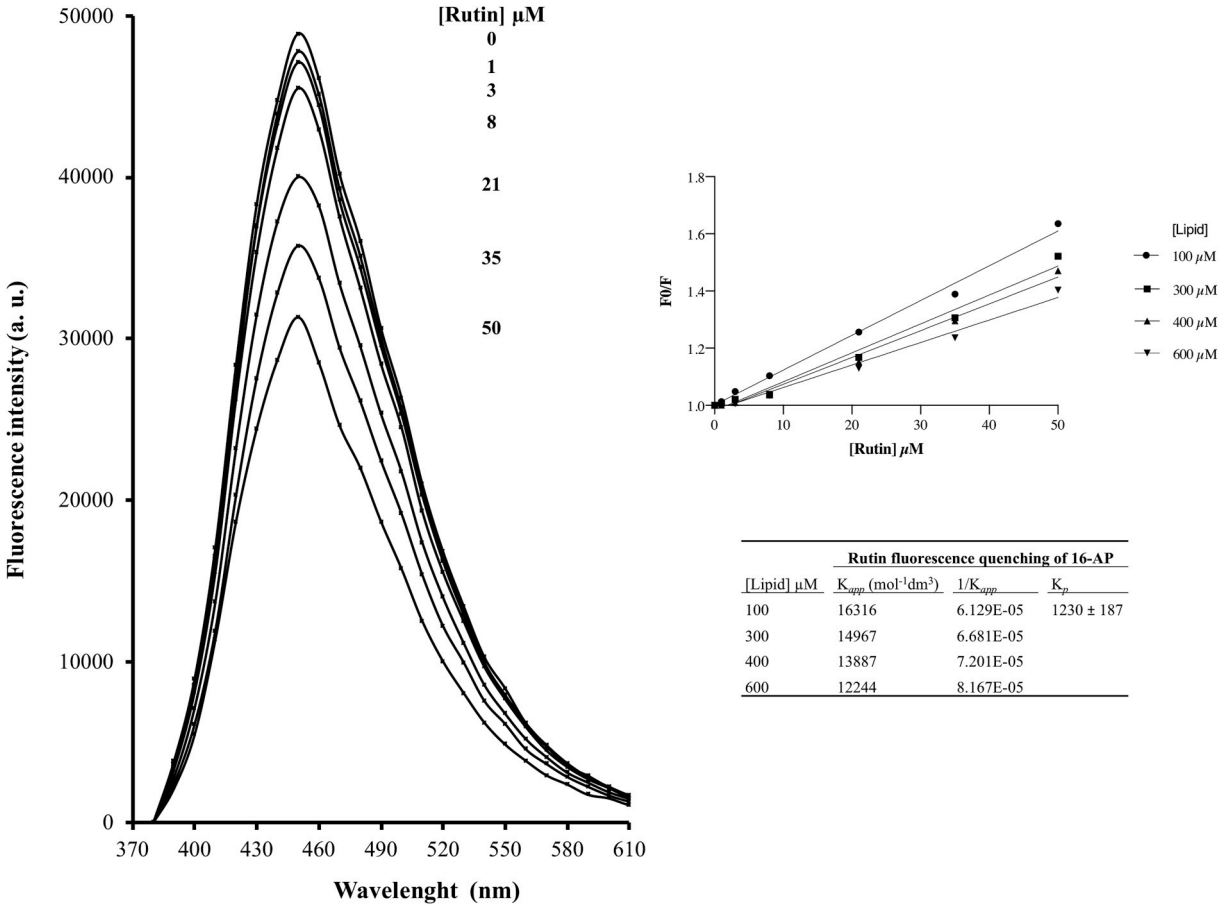

Rutin fluorescence quenching of 16-AP			
[Lipid] μM	K_{app} (mol^{-1}dm^3)	1/K_{app}	K_p
100	16316	6.129E-05	1230 ± 187
300	14967	6.681E-05	
400	13887	7.201E-05	
600	12244	8.167E-05	

Fig. 4. Fluorescence emission spectra (λ_{exc} = 365 nm) of 16-AP probe incorporated in liposomes (100 μM of lipid from the phospholipid-rich fraction) in the absence and presence of increasing concentrations of rutin (1–50 μM). In the inserted graphic are the Stern-Volmer plots from steady-state fluorescence measurements with 16-AP incorporated in increasing lipid concentrations (100–600 μM) as function of rutin concentration (0, 1, 3, 8, 16, 21, 35 and 50 μM). In the inserted table are the calculated values of the Apparent Stern-Volmer Constant (K_{app}) and of the partition coefficient (K_p) of rutin incorporated in liposomes, at 37 °C, at different lipid concentrations.

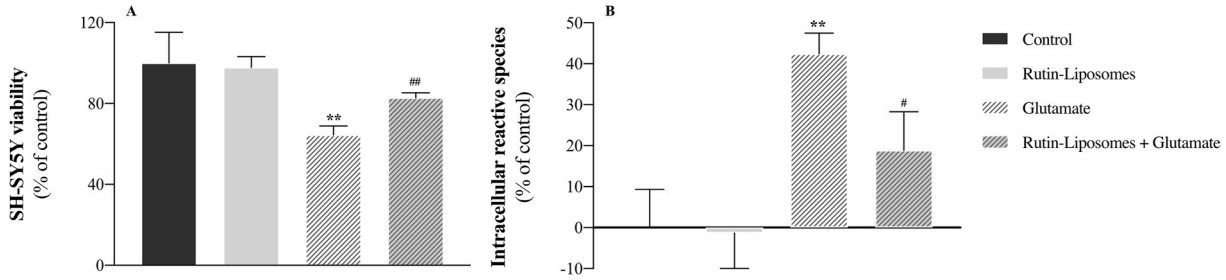

Fig. 5. *In vitro* assays with SH-SY5Y cells. (**A**) Assessment of SH-SY5Y viability by MTT reduction assay (0.5 mg/mL, 2 h at 510 nm) after 24 h of direct exposure to rutin-liposomes (lipid 25 μM + rutin 16.7 μM), to glutamate (50 mM), and pre-exposition to rutin-liposomes for 2 h followed by a 22 h of co-exposition with the toxicant. (**B**) Formation of intracellular reactive species triggered by glutamate (50 mM), and protective effect of rutin-liposomes (lipid 25 μM + rutin 16.7 μM); cells were pre-incubated with DCFH-DA (25 mM, 1 h), and toxicity was induced over 1 h, with and without pre-exposition to rutin-liposomes (2 h). The results were expressed as mean ± SD from triplicates of three independent experiments. The statistical analysis was performed with one-way ANOVA followed by Tukey's *post hoc* (level of statistical significance $*p < 0.05$). **, significantly different from control (untreated cells), with $p < 0.01$; # and ##, significantly different from the cells exposed to glutamate with $p < 0.01$ and $p < 0.05$, respectively.

oxidative stress, but without statistical significance (Fig. 5B). These results suggest that the ability of the nanoformulation to reduce the formation of intracellular reactive species may, in part, help attenuating the glutamate-induced toxicity.

Therefore, these rutin-liposomes functional nanoformulations, may come as an interesting strategy to take profit of the pharmacological properties of this bioactive flavonoid, with potential application within the field of neuroprotective agents.

4. Conclusion

The outlined experimental procedure allowed to extract phospholipids from egg yolk using only ethanol and acetone, following the European guidelines for extraction solvents used in the production of foodstuffs and food ingredients. With this procedure are obtained phospholipid-rich extracts of high purity degree without compromising the extraction yields. It was also designed to minimize the consumption of solvents by recovering ethanol for continuum extraction cycles. Therefore, the procedure aggregates valuable features for a possible industrial scale-up. Additionally, the main by-products cholesterol and carotenoids are obtained in separated acetone solutions, thus allowing their further application. Finally, the phospholipid-rich fraction was used to produce bioactive rutin-liposomes. Since phospholipid-rich extracts exhibit an interesting fatty acid profile, and their extractants do not raise objections to subsequent food and pharmaceutical applications, this is a promising methodology to develop new functional lipid-based products.

Acknowledgements

The work was supported by UID/QUI/50006/2019 with funding from FCT/MCTES through national funds, and by Programa de Cooperación Interreg V-A España – Portugal (POCTEP) 2014–2020 (project 0377_IBERPHENOL_6_E). The authors are greatly indebted to all financing sources. João Bernardo (SFRH/BD/129499/2017) thanks FCT/MCTES for his grant.

Appendix A. Supplementary data

Supplementary data to this article can be found online at https://doi.org/10.1016/j.fct.2019.110749.

References

Andrade, P.B., Grosso, C., Valentão, P., Bernardo, J., 2016. Flavonoids in neurodegeneration: limitations and strategies to cross CNS barriers. Curr. Med. Chem. 23, 4151–4174. https://doi.org/10.2174/0929867323666160809094934.

Anton, M., 2013. Egg yolk: structures, functionalities and processes. J. Sci. Food Agric. 93, 2871–2880. https://doi.org/10.1002/jsfa.6247.

Arora, A., Byrem, T.M., Nair, M.G., Strasburg, G.M., 2000. Modulation of liposomal membrane fluidity by flavonoids and isoflavonoids. Arch. Biochem. Biophys. 373, 102–109. https://doi.org/10.1006/abbi.1999.1525.

Atlante, A., Calissano, P., Bobba, A., Giannattasio, S., Marra, E., Passarella, S., 2001. Glutamate neurotoxicity, oxidative stress and mitochondria. FEBS Lett. 497, 1–5. https://doi.org/10.1016/S0014-5793(01)02437-1.

Bartlett, E.M., Lewis, D.H., 1970. Spectrophotometric determination of phosphate esters in the presence and absence of orthophosphate. Anal. Biochem. 36, 159–167. https://doi.org/10.1016/0003-2697(70)90343-X.

Bernardo, J., Ferreres, F., Gil-Izquierdo, Á., Valentão, P., Andrade, P.B., 2017. Medicinal species as MTDLs: *Turnera diffusa* Willd. Ex Schult inhibits CNS enzymes and delays glutamate excitotoxicity in SH-SY5Y cells via oxidative damage. Food Chem. Toxicol. 106, 466–476. https://doi.org/10.1016/j.fct.2017.06.014.

Briuglia, M.L., Rotella, C., McFarlane, A., Lamprou, D.A., 2015. Influence of cholesterol on liposome stability and on *in vitro* drug release. Drug Deliv. Transl. Res. 5, 231–242. https://doi.org/10.1007/s13346-015-0220-8.

Cassano, T., Pace, L., Bedse, G., Michele Lavecchia, A., De Marco, F., Gaetani, S., Serviddio, G., 2016. Glutamate and mitochondria: two prominent players in the oxidative stress-induced neurodegeneration. Curr. Alzheimer Res. 13, 185–197. https://doi.org/10.2174/1567205013666151218132725.

Du, M., Ahn, D.U., Sell, J.L., 1999. Effect of dietary conjugated linoleic acid on the composition of egg yolk lipids. Poult. Sci. 78, 1639–1645. https://doi.org/10.1093/ps/78.11.1639.

Enogieru, A.B., Haylett, W., Hiss, D.C., Bardien, S., Ekpo, O.E., 2018. Rutin as a potent antioxidant: implications for neurodegenerative disorders. Oxid. Med. Cell. Longev. https://doi.org/10.1155/2018/6241017.

European Council, 2009. Directive 2009/32/EC of the European Parliament and of the Councilon on the approximation of the laws of the Member States on extraction solvents used in the production of foodstuffs and food ingredients. Off. J. Eur. Union L41. https://doi.org/10.3000/19770677.L_2013.124.eng.

Fato, R., Battino, M., Esposti, M.D., Castelli, G.P., Lenaz, G., 1986. Determination of partition and lateral diffusion coefficients of ubiquinones by fluorescence quenching of n-(9-Anthroyloxy)stearic acids in phospholipid vesicles and mitochondrial membranes. Biochemistry 25, 3378–3390. https://doi.org/10.1021/bi00359a043.

Folch, J., Lees, M., Stanley, G.H.S., 1957. A simple method for the isolation and purification of total lipides from animal tissues. J. Biol. Chem. 226, 497–509. https://doi.org/10.1007/s10858-011-9570-9.

Gładkowski, W., Chojnacka, A., Kiełbowicz, G., Trziszka, T., Wawrzeńczyk, C., 2012. Isolation of pure phospholipid fraction from egg yolk. JAOCS, J. Am. Oil Chem. Soc. 89, 179–182. https://doi.org/10.1007/s11746-011-1893-x.

Gruszecki, W.I., Strzałka, K., 2005. Carotenoids as modulators of lipid membrane physical properties. Biochim. Biophys. Acta 1740, 108–115. https://doi.org/10.1016/j.bbadis.2004.11.015.

Gullón, B., Lú-Chau, T.A., Moreira, M.T., Lema, J.M., Eibes, G., 2017. Rutin: a review on extraction, identification and purification methods, biological activities and approaches to enhance its bioavailability. Trends Food Sci. Technol. 67, 220–235. https://doi.org/10.1016/j.tifs.2017.07.008.

Handa, T., Matsuzaki, K., Nakagaki, M., 1987. Orientations of a bifunctional molecule, 16-(9-anthroyloxy)palmitic acid, in micelles and liposomes. J. Colloid Interface Sci. 16, 50–58. https://doi.org/10.1016/0021-9797(87)90097-X.

Hawke, J.C., 1959. The fatty acids of phosphatidylethanolamine and phosphatidylcholine from hen's egg. Biochem. J. 71, 588–592.

Huang, M., Su, E., Zheng, F., Tan, C., 2017. Encapsulation of flavonoids in liposomal delivery systems: the case of quercetin, kaempferol and luteolin. Food Funct. 8, 3198–3208. https://doi.org/10.1039/c7fo00508c.

Huang, T.C., Chen, C.P., Wefler, V., Raftery, A., 1961. A stable reagent for the Liebermann-Burchard reaction: application to rapid serum cholesterol determination. Anal. Chem. 33, 1405–1407. https://doi.org/10.1021/ac60178a040.

Kovalcuks, A., Duma, M., 2016. Distribution of phospholipids, cholesterol and carotenoids in two-solvent system during egg yolk oil solvent extraction. World Acad. Sci. Eng. Technol. Int. J. Biol. Biomol. Agric. Food Biotechnol. Eng. 10, 323–328.

Mendes, D., Oliveira, M.M., Moreira, P.I., Coutinho, J., Nunes, F.M., Pereira, D.M., Valentão, P., Andrade, P.B., Videira, R.A., 2018. Beneficial effects of white wine polyphenols-enriched diet on Alzheimer's disease-like pathology. J. Nutr. Biochem. 55, 165–177. https://doi.org/10.1016/j.jnutbio.2018.02.001.

Mishra, D.K., Shandilya, R., Mishra, P.K., 2018. Lipid based nanocarriers: a translational perspective. Nanomed. Nanotechnol. Biol. Med. 14, 2023–2050. https://doi.org/10.1016/j.nano.2018.05.021.

Müller, R.H., Jacobs, C., Kayser, O., 2001. Nanosuspensions as particulate drug formulations in therapy: rationale for development and what we can expect for the future. Adv. Drug Deliv. Rev. 47, 3–19. https://doi.org/10.1016/S0169-409X(00)00118-6.

Nielsen, H., Shukla, V.K.S., 2004. *In situ* solid phase extraction of lipids from spray-dried egg yolk by ethanol with subsequent removal of triacylglycerols by cold temperature crystallization. LWT - Food Sci. Technol. (Lebensmittel-Wissenschaft -Technol.) 37, 613–618. https://doi.org/10.1016/j.lwt.2003.12.007.

Oliveira, A.P., Lobo-Da-Cunha, A., Taveira, M., Ferreira, M., Valentão, P., Andrade, P.B., 2015. Digestive gland from *Aplysia depilans* Gmelin: leads for inflammation treatment. Molecules 20, 15766–15780. https://doi.org/10.3390/molecules200915766.

Palacios, L.E., Wang, T., 2005. Egg-yolk lipid fractionation and lecithin characterization. JAOCS, J. Am. Oil Chem. Soc. 82, 571–578. https://doi.org/10.1007/s11746-005-1111-4.

Parkinson, T.L., 1966. The chemical composition of eggs. J. Sci. Food Agric. 17, 101–111. http://doi.org/10.1002/jsfa.2740170301.

Pimentel, L., Fontes, A.L., Salsinha, S., Machado, M., Correia, I., Gomes, A.M., Pintado, M., Rodríguez-Alcalá, L.M., 2018. Suitable simple and fast methods for selective isolation of phospholipids as a tool for their analysis. Electrophoresis 39, 1835–1845. https://doi.org/10.1002/elps.201700425.

Popova, A.V., Andreeva, A.S., 2013. Carotenoid-lipid interactions. Adv. Planar Lipid Bilayers Liposomes 17, 215–236. https://doi.org/10.1016/B978-0-12-411516-3.00008-5.

Rodriguez-Concepcion, M., Avalos, J., Bonet, M.L., Boronat, A., Gomez-Gomez, L., Hornero-Mendez, D., Limon, M.C., Meléndez-Martínez, A.J., Olmedilla-Alonso, B., Palou, A., Ribot, J., Rodrigo, M.J., Zacarias, L., Zhu, C., 2018. A global perspective on carotenoids: metabolism, biotechnology, and benefits for nutrition and health. Prog. Lipid Res. 70, 62–93. https://doi.org/10.1016/j.plipres.2018.04.004.

Rosa, D., Catalá, A., 1998. Fatty acid profiles and non enzymatic lipid peroxidation of microsomes and mitochondria from bovine liver, kidney, lung and heart. Arch. Physiol. Biochem. 106, 33–37. http://doi.org/10.1067/apab.106.1.33.4398.

Rowe, E.S., 1983. Lipid chain length and temperature dependence of ethanol-phosphatidylcholine interactions. Biochemistry 22, 3299–3305. https://doi.org/10.1021/bi00283a001.

Schlatterer, J., Breithaupt, D.E., 2006. Xanthophylls in commercial egg yolks: quantification and identification by HPLC and LC-(APCI)MS using a C30 phase. J. Agric. Food Chem. 54, 2267–2273. https://doi.org/10.1021/jf053204d.

Shukla, S., Haldorai, Y., Hwang, S.K., Bajpai, V.K., Huh, Y.S., Han, Y.K., 2017. Current demands for food-approved liposome nanoparticles in food and safety sector. Front. Microbiol. 8. https://doi.org/10.3389/fmicb.2017.02398.

Singh, R.P., Gangadharappa, H.V., Mruthunjaya, K., 2017. Phospholipids: unique carriers for drug delivery systems. J. Drug Deliv. Sci. Technol. 39, 166–179. https://doi.org/10.1016/j.jddst.2017.03.027.

Su, Y., Tian, Y., Yan, R., Wang, C., Niu, F., Yang, Y., 2014. Study on a novel process for the separation of phospholipids, triacylglycerol and cholesterol from egg yolk. J. Food Sci. Technol. 52, 4586–4592. https://doi.org/10.1007/s13197-014-1513-5.

Surai, P.F., Sparks, N.H.C., 2001. Designer eggs: from improvement of egg composition to functional food. Trends Food Sci. Technol. 12, 7–16. https://doi.org/10.1016/S0924-2244(01)00048-6.

Tan, C., Xue, J., Abbas, S., Feng, B., Zhang, X., Xia, S., 2014. Liposome as a delivery system for carotenoids: comparative antioxidant activity of carotenoids as measured by ferric reducing antioxidant power, DPPH assay and lipid peroxidation. J. Agric. Food Chem. 62, 6726–6735. https://doi.org/10.1021/jf405622f.

Videira, R.A., Antunes-Madeira, M.C., Madeira, V.M.C., 1999. Biophysical perturbations induced by ethylazinphos in lipid membranes. Chem. Phys. Lipids 97, 139–153. https://doi.org/10.1016/S0009-3084(98)00105-4.

Vilamarim, R., Bernardo, J., Videira, R.A., Valentão, P., Veiga, F., Andrade, P.B., 2018. An egg yolk's phospholipid-pennyroyal nootropic nanoformulation modulates monoamino oxidase-A (MAO-A) activity in SH-SY5Y neuronal model. J. Funct. Foods 46, 335–344. https://doi.org/10.1016/j.jff.2018.05.009.

White, S.H., Jacobs, R.E., King, G.I., 1987. Partial specific volumes of lipid and water in mixtures of egg lecithin and water. Biophys. J. 52, 663–665. https://doi.org/10.1016/S0006-3495(87)83259-9.